Rev. Roum. Sci. Techn.– Électrotechn. et Énerg.
Vol. **69**, *1*, pp. 91–96, Bucarest, 2024

STRUCTURED H_∞ CONTROL-BASED ROBUST POWER SYSTEM STABILIZER FOR STABILITY OF MULTI-MACHINE SYSTEM

ABDESLEM KHELLOUFI[1], BILAL SARI[1], SEIF EDDINE CHOUABA[2]

Keywords: Multi-machine system; Power system stabilizer; Structured H_∞ synthesis; Robust control.

A robust design of power system stabilizers (PSSs) using H_∞ output feedback control has been introduced in this work. To facilitate the implementation of the designed PSSs, the proposed technique employs the H_∞ to tune the fixed-structure conventional lead-lag PSS parameters of the multi-machine system. These PSSs are used to improve the damping of the local and inter-area low-frequency oscillations in power systems under different operating conditions. The proposed control is tested on a multi-machine system, which is a three-machine nine-bus system. A comparative simulation study shows a significant enhancement and good performance of the proposed design compared to an IEEE conventional power system stabilizer.

1. INTRODUCTION

The stability of power systems is one of the biggest challenges, the instability can lead to blackouts.

The low-frequency electromechanical oscillations are a serious problem in power system stability. The power system stabilizer (PSS) is an effective way to improve the damping of these oscillations, which is used to produce a supplementary signal through the excitation system [1–3].

The lead-lag phase compensator is the base of the conventional power system stabilizers.

The current IEEE standard [4] has classified the type of power system stabilizers according to the number of inputs in two categories: single-input like (PSS1A, PSS5C) and dual-input like (PSS2C, PSS3C, PSS4C, PSS6C, PSS7C). Also, the standard has classified according to the bands of the working frequency into two types: single frequency bands like (PSS1A, PSS2C...), and multiple frequency bands like (PSS4C, and PSS5C) which are used to damp separate frequency bands (very low, low, intermediate, and high-frequency modes) [4].

In the literature, different techniques have been designed to damp low-frequency oscillations.

The sliding mode control (SMC) is presented in paper [5], a farmland fertility algorithm (FFA) in [6] but the FFA is highly reliant on accurate and extensive data which can be challenging to acquire, a genetic algorithm in [7] which requires many iterations and evaluations, making it slow for complex problems like multi-machine system, a particle swarm optimization (PSO) in [8] but this algorithm performance critically depends on fine-tuning parameters, making it complex and less robust, a chaotic sunflower optimization algorithm in [9] which requiring careful tuning of chaotic parameters, struggles with local optima, prioritizing exploitation (refining good solutions) over exploration (finding new, potentially better regions) leading to missed global optima, a moth search algorithm in [10] but it lacks the rigorous mathematical backing of some established optimization methods, raising concerns about stability and global convergence guarantees, bio-inspired algorithms in [11] which is highly dependent on fine-tuning specific parameters, impacting effectiveness and requiring more expertise, a sliding mode control in [12]. Moreover, artificial intelligence-based training and tuning techniques have been used to develop a PSS as a Deep reinforcement learning-based method in [13], a neuro-adaptive predictive control in [14], a fuzzy-based controller in [15–17], damped Nyquist plot for the phase and gain optimization in [18] but all these algorithms may require intensive computations compared to simpler algorithms, especially for complex problems. Furthermore, robust control theories have been employed in the design of H_∞-based robust power system stabilizers [19] in the case of one machine connected to the electrical grid. It is noted that H_∞ control is inherently robust, providing stability and performance guarantees even in the presence of uncertainties and disturbances. Unlike some optimization methods which may rely on specific models, the H_∞ method utilizes a systematic approach that considers worst-case scenarios, making it suitable for a wide range of complex systems. Moreover, the H_∞ approach excels in addressing uncertainties and variations in system dynamics, ensuring stability and performance under diverse operating conditions. Besides, it is effective in dealing with time-varying systems, offering a reliable solution for dynamic processes that evolve.

At the nominal operating conditions, the conventional power system stabilizer (CPSS) works efficiently, but its performance decreases if the operating point has changed [20]. In this case, the CPSS does not guarantee the power system robustness for different ranges of operating points.

To solve the robustness problem, the robust control design guarantees stability under external disturbance or parametric uncertainties. In [21], the authors have designed their PSS using the concept of Glover-McFarlane's loop shaping design, but it is applied only in the case of one machine connected to the infinite bus. A linear matrix inequalities (LMI) technique is used to synthesize a state feedback robust PSS using pole-placement [22] but it assumes all the system states are measurable which is not the case in an industrial context.

Robust control methods based on H_2 and H_∞ Norm designed in [19,20] have been only applied on an SMIB.

In this work, a structured H_∞ control approach has been developed to tune control block parameters of conventional CPSS on the Multi-Machine system with two weighting functions. This is the main contribution of this paper. Besides to the authors' knowledge, this work is not in the literature. Compared to other optimization methods like genetic algorithms (GA), particle swarm optimization (PSO), and others used for control system design, the H-infinity method offers several advantages. These include robustness to uncertainties, stability guarantees, and computational efficiency. These features make H_∞ control a powerful tool for controlling complex systems in the presence of uncertainties and disturbances.

[1] Electrical Engineering Department, University of Setif 1, Algeria. E-mail:Abdeslem.khelloufi@univ-setif.dz, Bilal.sari@univ-setif.dz
[2] DAC Laboratory, University of Setif 1, Algeria. E-mail: Seif.chouaba@univ-setif.dz

DOI: 10.59277/RRST-EE.2024.69.1.16

This paper is organized as follows. Section 2 presents the description and mathematical model of the multi-machine system. Section 3 gives the structured H∞ control design. Section 4 explains the proposed resolution and the chosen weighting functions in the proposed design. Section 5 shows the simulation results, in which a comparative study is performed between the proposed control strategy and the conventional CPSS. Finally, Section 6 ends this paper and gives some concluding observations.

2. PLANT MODEL

The dynamic stability of Multi-Machine power systems can be described by a set of nonlinear differential equations. A multi-machine system of this study consists of three machines and nine buses, as shown in Fig.1. The system data are given in [23].

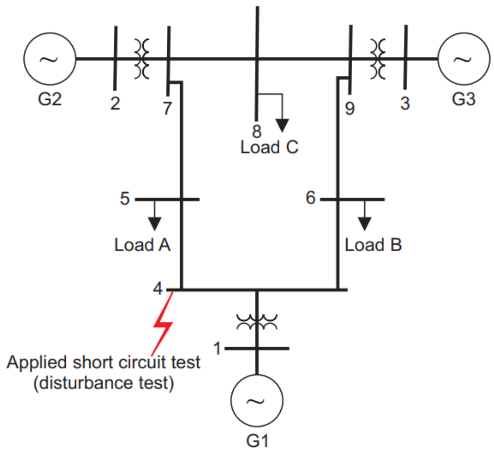

Fig. 1 – Diagram of nine-bus system.

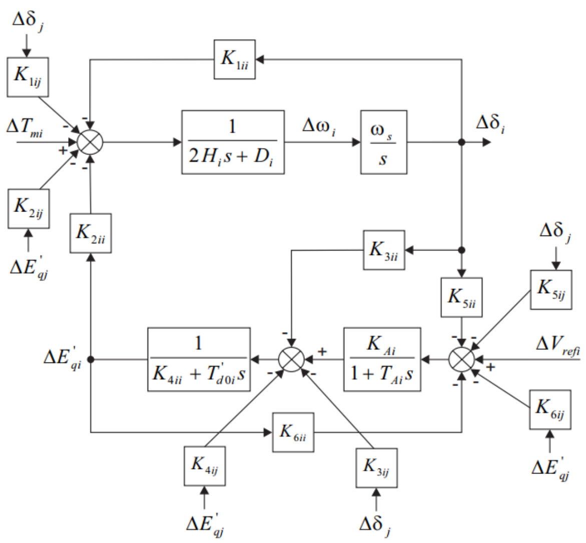

Fig. 2 – A linear model of a multi-machine power system.

The nonlinear mathematical model of the system is described by the equations given below:

$$\dot{\delta}_i = (\omega_i - \omega_s), \tag{1}$$

$$\dot{\omega}_i = \frac{\omega_s}{2H_i}\left[T_{mi} - T_{ei} - D_i(\omega_i - \omega_s)\right], \tag{2}$$

$$\dot{E}'_{qi} = \frac{1}{T'_{doi}}\left[E'_{qi} + (X_{di} - X'_{di})I_{di} - E_{fdi}\right], \tag{3}$$

$$\dot{E}'_{fdi} = \frac{1}{T_{Ai}}\left[-E_{fdi} + K_{Ai}\left(V_{refi} - V_{ti}\right)\right], \tag{4}$$

$$T_{ei} = E'_{qi}I_{qi} - \left(X_{qi} - X'_{di}\right)I_{di}I_{qi}, \tag{5}$$

where all the model parameters are given in the nomenclature.

The scheme of the linear model [24] of the multi-machine system is shown in Fig. 2.

The linearized state-space model can be written as:

$$\Delta\dot{x}(t) = A\Delta x(t) + B_1\Delta w(t) + B_2\Delta u(t),$$
$$\Delta y(t) = C\Delta x(t), \tag{6}$$

where $\Delta x(t)$ is the state vector, $\Delta w(t)$ is a vector of the external inputs (Reference voltages and mechanical torques), the control signal of the power system stabilizer $\Delta u(t)$, and the system output signal is Δy. The main matrices A, B_1, B_2, C can be found in [24].

As the conventional PSS (CPSS) is widely used in industrial power plants with fixed structures and to facilitate the implementation of the proposed advanced PSSs, this paper focuses on the tuning blocks of CPSS by using a fixed-structure H∞ control design approach. The fixed structure of CPSSs is written under the following form [4]:

$$K_2(s) = K_{s2}\frac{T_{w2}s}{(1+T_{w2}s)}\frac{(1+T_{12}s)(1+T_{32}s)}{(1+T_{22}s)(1+T_{42}s)}, \tag{7}$$

$$K_3(s) = K_{s3}\frac{T_{w3}s}{(1+T_{w3}s)}\frac{(1+T_{13}s)(1+T_{33}s)}{(1+T_{23}s)(1+T_{43}s)}, \tag{8}$$

where K_{s2} and K_{s3} are the PSS gains, T_{w2} and T_{w3} are wash-out time constants, T_{1i}, T_{2i}, T_{3i}, and T_{4i} are time constants of the i^{th} generator.

3. STRUCTURED H∞ CONTROL DESIGN

The structured H∞ control technique is used to tune control block parameters, it is a special case of H∞ synthesis [25,26]. In this paper, the tuning control block parameters of conventional CPSS is performed by using structured H∞ synthesis. The representation of the problem is illustrated in Fig. 3, where the augmented plant transfer matrix is $P(s)$ which combines fixed parameters.

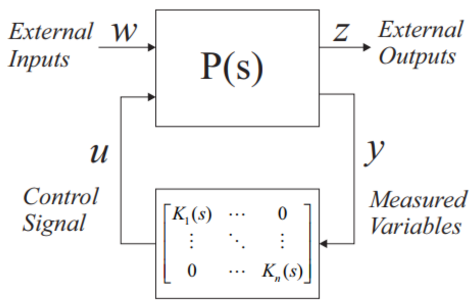

Fig. 3 – Standard representation for structured H_∞ synthesis.

The robust structured HPSS controller is $K(s)$ which combines tunable parameters (K_{si}, T_{1i}, T_{2i}, T_{3i}, T_{4i}) of conventional CPSS. The external inputs w are the reference voltage variations (ΔV_{ref1}, ΔV_{ref2}, and ΔV_{ref3}) and the mechanical torque variations (ΔT_{m1}, ΔT_{m2}, and ΔT_{m3}) of the generators G1, G2, and G3 respectively. The measurement outputs y are the speed deviations ($\Delta\omega_2$ and $\Delta\omega_3$) of the generators G2 and G3 respectively. The control signals u are the outputs of proposed H∞ power system stabilizers (HPSS2 and HPSS3) and the external outputs z are chosen to be the variation of speed deviations $\Delta\omega_{12}$ of the generators $G1$, $G2$ and $\Delta\omega_{13}$ of the generators $G1$, $G3$. These external signals z will be filtered by some weighting functions before their use in the H_∞ optimization problem. More details about the used weighting functions will be given in the next section.

The structured H_∞ synthesis is based on minimization of the H_∞ norm as follows:

$$\|H(s)\|_\infty = \max_\omega \overline{\sigma}\big(H(\mathrm{j}\omega)\big) \le \gamma, \tag{9}$$

where $\overline{\sigma}$ is the maximum singular value, and γ is the H_∞ norm to be minimized.

The linear fractional transformation (LFT) representation for H_∞ is given as follows:

$$H(s) = F_l\big(P(s), \mathrm{Diag}(K_1(s),\ldots,K_1(s))\big), \tag{10}$$

where F_l represents the lower LFT representation and Diag represents a diagonal block of $K_i(s)$.

The open-loop transfer matrix from $\begin{bmatrix} z \\ y \end{bmatrix}$ to $\begin{bmatrix} w \\ u \end{bmatrix}$ is given as follows:

$$\begin{bmatrix} z \\ y \end{bmatrix} = \begin{bmatrix} P_{11}(s) & P_{12}(s) \\ P_{21}(s) & P_{22}(s) \end{bmatrix} \begin{bmatrix} w \\ u \end{bmatrix}, \tag{11}$$

The linear fractional transformation (LFT) representation of the system in closed loop is given as follows:

$$T_{zw}(s) = P_{11} + P_{12}K[(I - P_{22})K]^{-1}. \tag{12}$$

4. H_∞ CONTROLLER RESOLVING

It is necessary to include some weighting functions $W_1(s)$ and $W_2(s)$ in the Plant to get some dynamical performances in an H_∞ problem. Figure 4 illustrates the augmented plant with the weighting functions $W_1(s)$ and $W_2(s)$. The new considered external outputs are: z_1 and z_2, where z_1 is the variation of speed deviations $\Delta\omega_1$ and $\Delta\omega_2$ connected to weighting function W_1($z_1 = W_1(s)\Delta\omega_{12}$) and z_2 is the variation of speed deviations $\Delta\omega_1$ and $\Delta\omega_3$ connected to weighting function W_2($z_2 = W_2(s)\,\Delta\omega_{13}$).

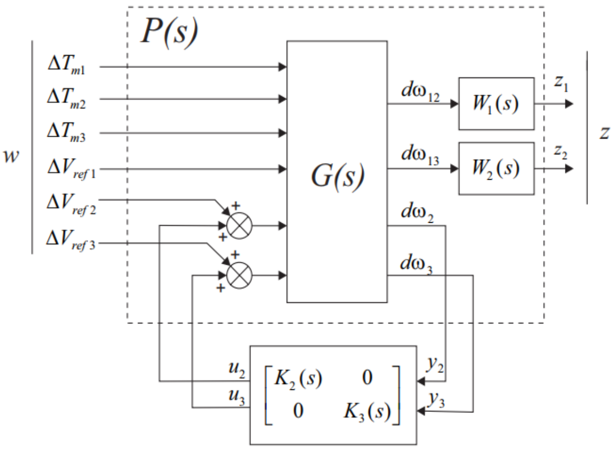

Fig. 4 – Weighting functions augmentation of the system.

The choice of these weighting functions is an essential step. The structures of weighting functions $W_1(s)$ and $W_2(s)$ are given by the following equations:

$$W_1(s) = \frac{M_1 s + w_{b1}}{s + w_{b1}\varepsilon_1}, \tag{13}$$

$$W_2(s) = \frac{M_2 s + w_{b2}}{s + w_{b2}\varepsilon_2}, \tag{14}$$

where M_i, w_{bi} and ε_i are the tuning parameters. The following values satisfy the performance requirements for the considered nominal operating point:

The first weighting function parameters are: M_1=110, w_{b1}=50 and ε_1=10^{-4} and the second weighting function parameters are: M_2=100, w_{b2} = 110 and ε_2=10^{-4}.

The obtained numerical values of tuned parameters' HPSSs are given in the Table 1.

5. SIMULATION RESULTS

To verify the effectiveness and the robustness of the proposed HPSS2 and HPSS3, several studies have been performed on the multi-machine system at different operating points where the data of the system and loading conditions are given in the Table 2 and Table 3. It is noted that “Light load” refers to operating the generator at a fraction of its rated capacity, typically less than 25 %. “Normal load” is the typical operating range for the generator, around 50-75 % of its rated capacity. “Heavy load” refers to running the generator at or near its full capacity, typically 75-100 % of its rated capacity.

Table 1

The HPSS2 and HPSS3 data

HPSS2		HPSS3	
Parameter	Value	Parameter	Value
K_{s2}	43.2826	K_{s3}	0.3280
T_{w2}	10.00	T_{w3}	10.00
T_{12}	0.18984	T_{13}	1.9980
T_{22}	0.00408	T_{23}	*0.0340*
T_{32}	0.19534	T_{33}	2.1973
T_{42}	0.00434	T_{43}	0.0390

Table 2

System operating conditions (in p.u.)

Generator	Light		Normal		Heavy	
	P	*Q*	*P*	*Q*	*P*	*Q*
G1	0.362	0.162	0.716	0.271	2.207	1.088
G2	0.800	-0.109	1.630	0.067	1.920	0.564
G3	0.450	-0.204	0.850	-0.107	1.280	0.359

Table 3

Loading conditions (in p.u.)

Load	Light		Normal		Heavy	
	P	*Q*	*P*	*Q*	*P*	*Q*
A	0.65	0.55	1.25	0.50	2.00	0.80
B	0.45	0.35	0.90	0.30	1.80	0.60
C	0.50	0.25	1.00	0.35	1.50	0.60

Furthermore, a comparative study is carried out with CPSSs [23], where a scenario of severe disturbance rejection test is considered. It consists of a standard three phases short circuit near the node 4 at t = 1s (see Fig. 1). After 50 ms, the line (4–5) is opened at t= 1.1s this line is closed.

Figures 5 to 7 present a system response using the conventional PSSs (CPSSs) and the proposed stabilizers (HPSSs) to a transient disturbance during nominal operating conditions.

Comparing the simulation results obtained with the HPSSs and with conventional CPSSs shows that the proposed stabilizers achieve good robustness and performances. As can be observed in Figs. 5–13. The Tables 4 and 5 show a quantitative comparison of the proposed HPSS with a conventional CPSS and without

PSSs. The Table 4 represents the first oscillation amplitude of the system response. It is noted that the proposed HPSSs gives smaller oscillation in all generators overall operating conditions. The Table 5 shows the settling time for $|\Delta\omega_i| < 1.5 \cdot 10^{-4}$. The proposed HPSSs gives a better settling time in all generators in a heavy load.

In nominal load, it gives a better settling time in two generators (G2 and G3). And in the light load, it gives a better settling time in the generator G2. Besides, the proposed HPSSs gives the best settling time in six out of the tested nine cases. The conventional CPSS gives a better settling time only in the three cases compared to the proposed HPSSs. Furthermore, the proposed HPSSs have the best dynamical performance in terms of oscillations damping.

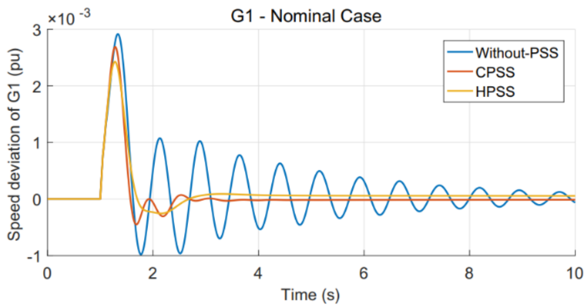

Fig. 5 – Speed deviation of generator 1 for nominal load.

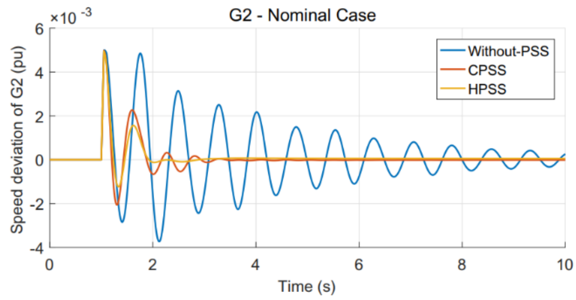

Fig. 6 – Speed deviation of generator 2 for nominal load.

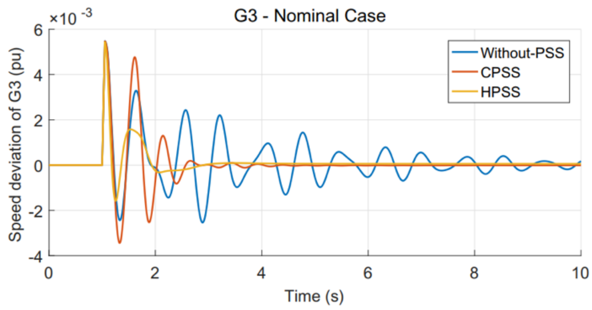

Fig. 7 – Speed deviation of generator 3 for nominal Load.

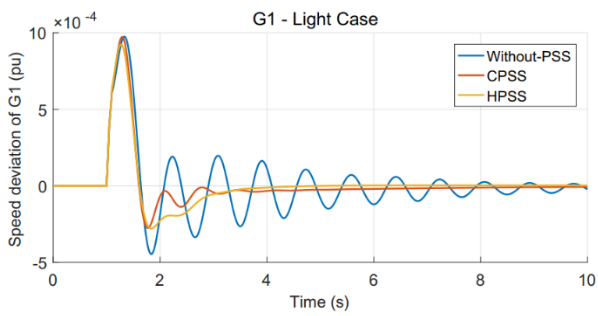

Fig. 8 – Speed deviation of generator 1 for light load.

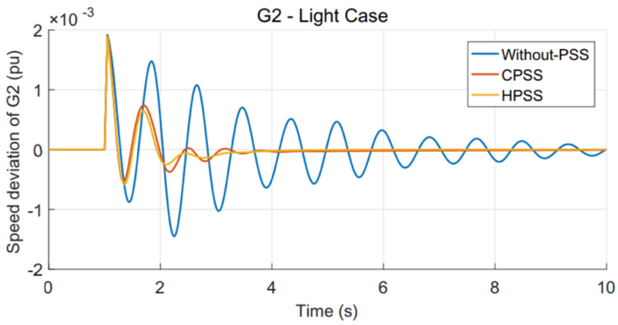

Fig. 9 – Speed deviation of generator 2 for light load.

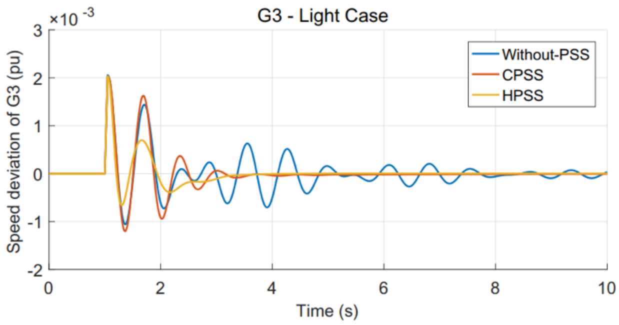

Fig. 10 – Speed deviation of generator 3 for light load.

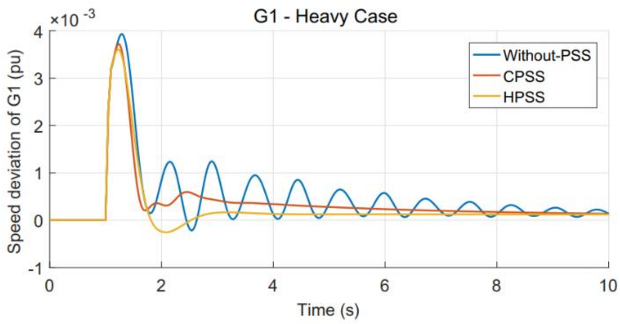

Fig. 11 – Speed deviation of generator 1 for heavy load.

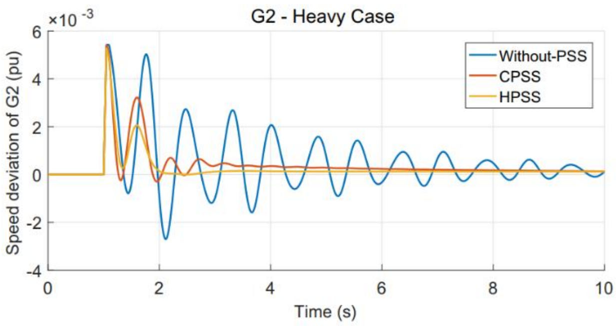

Fig. 12 – Speed deviation of generator 2 for heavy load.

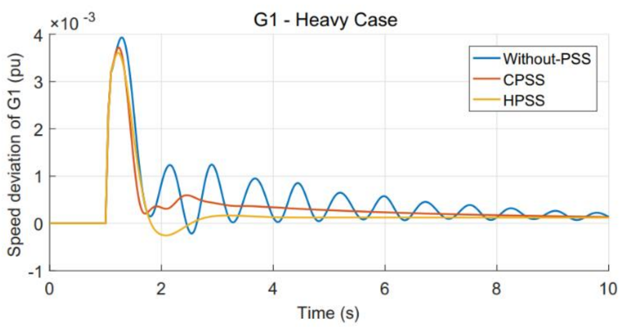

Fig. 13 – Speed deviation of generator 3 for heavy load.

Table 4

Comparison of 1st oscillation amplitude between the conventional PSSs (CPSSs) and the proposed PSS (HPSSs)

Case	PSS Type	*G1*	*G2*	*G3*
Nominal	Without-PSS	2.918	4.994	5.740
Load	CPSSs	2.689	4.976	5.467
in 10^{-3} p.u.	HPSSs	**2.427**	**4.951**	**5.438**
Light	Without-PSS	0.974	1.920	2.053
Load	CPSSs	0.972	1.896	2.031
in 10^{-3} p.u.	HPSSs	**0.923**	**1.885**	**2.029**
Heavy	Without-PSS	3.931	5.422	7.681
Load	CPSSs	3.719	5.410	7.670
in 10^{-3} p.u.	HPSSs	**3.606**	**5.274**	**7.456**

Table 5

Comparison of the settling time between the conventional PSSs (CPSSs) and the proposed PSS (HPSSs)

Case	PSS Type	*G1*	*G2*	*G3*
Nominal	Without-PSS	8.976	>10s	>10s
Load	CPSSs	**2.328**	2.845	2.706
in 10^{-3} p.u.	HPSSs	2.416	**1.877**	**2.641**
Light	Without-PSS	3.954	8.176	7.272
Load	CPSSs	**1.920**	2.902	**2.813**
in 10^{-3} p.u.	HPSSs	2.565	**2.264**	2.872
Heavy	Without-PSS	>10s	>10s	>10s
Load	CPSSs	9.085	9.102	9.053
in 10^{-3} p.u.	HPSSs	**3.601**	**1.996**	**3.629**

6. **CONCULSION**

In this paper, a robust power system stabilizer design using structured H_∞ synthesis is presented to enhance the stability and robustness of the multi-machine system. Three different operating points have been considered.

The proposed HPSS2 and HPSS3 controllers have a simple architecture, good performance and good robustness compared to the conventional CPSS.

The simulation results confirm the great benefit of the proposed HPSSs compared to the conventional CPSS regarding the stability, the disturbance rejection, and the speed deviation dynamical performances in several loading conditions.

APPENDIX

A. THE MULTI-MACHINE DATA

The parameters of the generators are given in Table A.1:

Table A.1

Loading conditions (in p.u.)

Generator	X_d	X'_d	T'_{do}	X_q	*H*	*D*
G1	0.1460	0.0608	8.9600	0.0969	23.64	9.6
G2	0.8958	0.1198	6.0000	0.8645	6.40	2.5
G3	1.3125	0.1813	5.8900	1.2578	3.01	1.0

B. THE SMIB DATA

The numerical values of parameters' CPSSs [4] are given in Table B.2.

Table B.2

The CPSS2 and CPSS3 data

CPSS2		CPSS3	
Parameter	Value	Parameter	Value
K_{s2}	2.4272	K_{s3}	0.3666
T_{w2}	10.00	T_{w3}	10.00
T_{12}	0.9728	T_{13}	0.9303
T_{22}	0.0500	T_{23}	*0.0500*
T_{32}	0.8417	T_{33}	1.5315
T_{42}	0.0500	T_{43}	0.0500

NOMENCLATURE

$()_i$	Generator i
H_i	Inertia constant (s)
ω_i	Rotor angular speed (rad/s)
ω_s	Synchronous rotor angular speed (rad/s)
δ_i	Power angle (rad)
I_{di}, I_{qi}	d and q-axis components (p.u.) of the i^{th} generator current
K_{Ai}, T_{Ai}	Gain (p.u.) and time constant (s) of AVR
E_{fdi}	Rotor field voltage (p.u.)
V_{ti}	Terminal voltage (p.u.)
V_{refi}	Reference voltage (p.u.)
T_{ei}, T_{mi}	Electrical and mechanical torque (p.u.)
E'_{qi}	q-axis transient internal voltage (p.u.)
T'_{doi}	d-axis transient open circuit generator time constant (s)
X_{di}, X_{qi}	Generator d and q-axis reactance (p.u.)
X'_{di}	Generator d-axis transient reactance (p.u.)
D_i	Damping coefficient
P,Q	Active and reactive powers (p.u.)
$K_{1ij},\ldots,K_{6ij}$	Linearized multi-machine system constants
K_{si}, T_{wi}, T_{ji}	Gain, washout time constant, and time constants of PSSs of the i^{th} generator
Gi	The i^{th} generator
PSS	Power System Stabilizer
CPSSi	The i^{th} conventional PSS
SMIB	Single Machine connected to Infinite Bus
HPSSi	The i^{th} proposed H_∞ PSS
u, y	The control signal and input signal of PSS

Received on 24 March 2023

REFERENCES

1. P. Kundur, N.J. Balu, M.G. Lauby, *Power System Stability and Control*, McGraw-hill New York, 1994.
2. A. Sallam, O.P. Malik, *Power system stability: modelling, analysis and control*, The Institution of Engineering and Technology, 2015.
3. S. Gurung, F. Jurado, S. Naetiladdanon, A. Sangswang, *Comparative analysis of probabilistic and deterministic approach to tune the power system stabilizers using the directional bat algorithm to improve system small-signal stability*, Electric Power Systems Research, **181** (2020).
4. IEEE, *Recommended Practice for Excitation System Models for Power System Stability Studies*, IEEE Std 421.5-2016 (Revision of IEEE Std 421.5-2005, pp. 1–207 (2016).
5. K.M. Sreedivya, P.A. Jeyanthy, D. Devaraj, *Design of power system stabilizer using sliding mode control technique for low frequency oscillations damping*, 2019 IEEE International Conference on Intelligent Techniques in Control, Optimization and Signal Processing (INCOS), Tamilnadu, India, pp. 1–6 (2019).
6. A. Sabo, N.I. Abdul Wahab, M.L. Othman, M.Z.A Mohd Jaffar, H. Beiranvand, *Optimal design of power system stabilizer for multimachine power system using farmland fertility algorithm*. International Transactions on Electrical Energy Systems, **30**, *12* (2020).
7. H. Labdelaoui, F. Boudjema, D. Boukhetala, *Multiobjective optimal design of dual-input power system stabilizer using genetic algorithms,* Roum. Sci. Techn. – Électrotechn. et Énerg., **62**, *1*, pp. 93–97 (2017).
8. G. Shahgholian, A. Mohavedi, *Coordinated design of thyristor-controlled series capacitor and power system stabilizer controllers using velocity update relaxation particle swarm optimization for two machine power system stability*, Rev. Roum. Sci. Techn. – Électrotechn. et Énerg., **59**, *3*, pp. 291–301 (2014).
9. B.M. Alshammari, T. Guesmi, *New chaotic sunflower optimization algorithm for optimal tuning of power system stabilizers,* Journal of Electrical Engineering & Technology, **15**, *5*, pp.1985–1997 (2020).
10. N. Razmjooy, S. Razmjooy, Z. Vahedi, V.V. Estrela, GG. de Oliveira, *A new design for robust control of power system stabilizer based on moth search algorithm*, Metaheuristics and Optimization in Computer and Electrical Engineering, 2021, pp.187–202.
11. E.L. Miotto, P.B. de Araujo, E. de Vargas Fortes, B.R. Gamino, L. Martins, *Coordinated tuning of the parameters of PSS and POD controllers using bioinspired algorithms,* IEEE Transactions on Industry Applications, **54**, *4*, pp.3845–3857 (2018).
12. A. Mourad, G. Keltoum, *Power system stabilizer based on terminal*

sliding mode control, Rev. Roum. Sci. Techn. – Électrotechn. et Énerg., **62**, *1*, pp. 98–102 (2017).
13. G. Zhang, W. Hu, D. Cao, Q. Huang, J. Yi, Z. Chen, F. Blaabjerg, *Deep reinforcement learning-based approach for proportional resonance power system stabilizer to prevent ultra-low-frequency oscillations,* IEEE Transactions on Smart Grid, **11**, *6*, pp. 5260-5272 (2020).
14. F. Jamsheed, S.J. Iqbal, *A minimal architecture neuro adaptive predictive control scheme for power system stabilizer*, International Journal of Electrical Power & Energy Systems, **137** (2022).
15. K.M. Sreedivya, P.A. Jeyanthy, D. Devaraj, *Improved design of interval type-2 fuzzy based wide area power system stabilizer for inter-area oscillation damping,* Microprocessors and Microsystems, **83** (2021).
16. P. Sahithya, N. Kumar, *Enhancement of Transient Stability of a SMIB System Using Fuzzy Logic-Based Power System Stabilize*r, in *Recent Advances in Power Systems*, Springer Nature Singapore, Singapore, pp. 311–319 (2022).
17. I. Dehiba, M. Abid, A. Aissaoui, *Robust design of power system stabilizer for a single generator-infinite bus power system,* Rev. Roum. Sci. Techn. – Électrotechn. et Énerg., **66**, *4*, pp. 249–253 (2021).
18. F. De Marco, P. Rullo, *Damped Nyquist plot for the phase and gain optimization of power system stabilizers*, Electric Power Systems Research, **205** (2022).
19. A. Khelloufi, B. Sari, S.E. Chouaba, *H∞ control based robust power system stabilizer for stability enhancement*, Rev. Roum. Sci. Techn. – Électrotechn. et Énerg., **67**, *2*, pp.175–180 (2022).
20. A. Sil, T. Gangopadhyay, S. Paul, A. Maitra, *Design of robust power system stabilizer using H∞ mixed sensitivity technique*, 2009 International Conference on Power Systems (IEEE), Kharagpur, India.
21. S. Barik, A.T. Mathew, *March.* *Design and comparison of power system stabilizer by conventional and robust H_∞ loop shaping technique,* 2014, International Conference on Circuits, Power and Computing Technologies, Nagercoil, India.
22. P.S. Rao, I. Sen, *Robust pole placement stabilizer design using linear matrix inequalities*, IEEE Transactions on Power Systems, **15**, *1*, pp. 313–319 (2000).
23. P.M. Anderson, A.A. Fouad, *Power system control and stability,* John Wiley & Sons, 2008.
24. Y.N. Yu, *Electric power system dynamics,* Academic Press, INC., New York, 1983.
25. P. Apkarian, D. Noll, *Nonsmooth H_∞ synthesis*, IEEE Transactions on Automatic Control, **51**, *1*, pp.71–86 (2006).
26. P. Gahinet, P. Apkarian, *Structured H∞ synthesis in MATLAB*, IFAC Proceedings, **44**, *1*, pp. 1435–1440 (2011).